Environmental Earth Sciences (2018) 77:550
https://doi.org/10.1007/s12665-018-7723-9

ORIGINAL ARTICLE

Climate change impacts on water demand and availability using CMIP5 models in the Jaguaribe basin, semi-arid Brazil

Rubens Gondim[1] · Cleiton Silveira[2] · Francisco de Souza Filho[3] · Francisco Vasconcelos Jr.[3] · Daniel Cid[3]

Received: 10 April 2017 / Accepted: 18 July 2018 / Published online: 27 July 2018

Abstract

The objective of this study was to analyze climate change impacts on irrigation water demand and availability in the Jaguaribe River basin, Brazil. For northeastern Brazil, five global circulation models were selected using a rainfall seasonal evaluation screening technique from the Intergovernmental Panel on Climate Change named *Coupled Model Intercomparison Project Phase 5*. The climate variables were generated for the base period of 1971–2000, as were projections for the 2025–2055 future time slice. Removal of maximum and minimum temperature and rainfall output bias was used to estimate reference evapotranspiration, irrigation water needs, and river flow using the rainfall—river flow hydrological model *Soil Moisture Accounting Procedure* for the baseline and future climate (*Representative Concentration Pathways* 4.5 and 8.5 scenarios). In addition, by applying improved irrigation efficiency, a scenario was evaluated in comparison with field observed performance. The water-deficit index was used as a water availability performance indicator. Future climate projections by all five models resulted in increases in future reference evapotranspiration (2.3–6.3%) and irrigation water needs (2.8–16.7%) for all scenarios. Regarding rainfall projections, both positive (4.8–12.5%) and negative (− 2.3 to − 15.2%) signals were observed. Most models and scenarios project that annual river flow will decrease. Lower future water availability was detected by the less positive water-deficit index. Improved irrigation efficiency is a key measure for the adaptation to higher future levels of water demand, as climate change impacts could be compensated by gains in irrigation efficiency (water demand changes varying from − 1.7 to − 35.2%).

Keywords Climate change · Irrigation · Hydrology · Jaguaribe

Introduction

Global climate modeling and advances in the physical climate process description and resolution have brought about better estimates and a reduction of uncertainties (Cubasch et al. 2013). The Intergovernmental Panel on Climate Change's (IPCC) 5th Assessment Report (AR5) called *Coupled Model Intercomparison Project Phase 5* (CMIP5) is based on global circulation models (GCMs) and state-of-the-art Earth system models (ESMs), and includes a representation of biogeochemical cycles and high-performance computers (Flato et al. 2013). The horizontal resolution assumes that a latitude and longitude of 1° represents approximately 111 km. It also includes a vertical resolution of the atmosphere up to 95 levels, which comprises a wide range of atmospheric processes. The CMIP5 model components include atmosphere (up to 52,000 horizontal grid points), land surface, ocean (up to 110,000 horizontal grid points), sea ice, aerosols, dynamic vegetation, atmospheric chemistry, carbon cycle, and ocean biogeochemistry cycles (Flato et al. 2013; Cubasch et al. 2013).

Higher temperatures due to climate change are expected to impact evapotranspiration, which affects water demand by crops. However, reservoir water inflow depends on rainfall and, thus, water availability for irrigation and other demand sectors. Climate change and food demand may act as additional drivers for water resource conflicts due to increasing water needs, especially for irrigated agriculture.

✉ Rubens Gondim
rubens.gondim@embrapa.br

[1] Embrapa Agroindústria Tropical, Rua Dra.Sara Mesquita 2270, Fortaleza, CE 60511-110, Brazil

[2] Unilab, Campus da Liberdade, Avenida da Abolição, 3-Centro, Redenção, CE CEP 62790-000, Brazil

[3] Departamento de Engenharia Hidráulica e Ambiental, Universidade Federal do Ceará, Bloco 713, 1.° Andar, Centro de Tecnologia, Fortaleza, CE CEP 60451-970, Brazil

Studies about climate change and irrigation water demand have been performed globally. Some have also simultaneously analyzed crop area growth as a result of the need to increase food production. Panagoulia and Bili (2002) found that net irrigation requirement increased for all scenarios (varying from 11 to 45%) in 45 cultivation areas and growing seasons due to higher evapotranspiration and crop coefficients. An increase in irrigated area was observed because of the change of the rain-fed system to irrigated crop. According to Panagoulia (2004), part of the water demand could be met by increasing irrigation efficiency, but a new water supply is needed in this case. Maeda et al. (2011) indicated that the total annual volume of the irrigation water required was likely to decrease in Eastern Kenya during the next 20 years. On the other hand, the tendency to expand agriculture is expected to aggravate water scarcity problems. No appreciable change in total irrigation water demand due to the shortening of the irrigation period for rice crops in Bangladesh was reported by Shahid (2011); however, climate change will increase the irrigation rate or daily use of water for irrigation, affecting the groundwater level. In addition, irrigation water demand impacted by climate change may vary by geographic location and environment peculiarities. Wada et al. (2013) reported results that ranged from slight decreases and increases to considerable increases in water irrigation demand, as higher greenhouse gas concentration scenarios were considered. The study also concluded that the magnitude of the increase depends on the degree of global warming and associated precipitation patterns. Valverde et al. (2015) concluded that climate change is expected to severely affect water requirements for irrigated agriculture in the Guadiana River basin, Portugal. A general increase in net irrigation requirements of the main representative crops was identified for the five different climate change scenarios. Hong et al. (2016) also reported an increase in the net irrigation requirement for cereals and vegetable crops in South Korea.

Some climate change assessments have also been done in the semi-arid northeastern region of Brazil. Krol and Bronstert (2007) obtained contradictory future rainfall projections. They also concluded that the agricultural water demand results could significantly vary based on the GCM applied. Gondim et al. (2012) concluded that irrigation water needs increased in the Jaguaribe basin by 7.9 and 9.1% over the period of 2025–2055 compared with the 1961–1990 baseline levels. Northeastern Brazil has historically high emigration rates due to a combination of severe drought periods and better labor opportunities in the Brazilian southeast. The impacts of climate change on the economic performance of the agriculture sector and on migration may create situations of socioeconomic vulnerability, which demand the design of appropriate adaptation policies (Barbieri et al. 2010). Regarding the Jaguaribe River basin, concerns with possible increased water demand require information to delineate adaptation policy strategies for future climate. The objective of this study was to identify climate change impacts on water availability and demand in the Jaguaribe River basin, Brazil, using rainfall seasonal evaluation performance as a screening technique to select IPCC CMIP5 GCMs, as well as to propose an adaptation policy for the irrigation sector.

Materials and methods

Study area

Ceará State, Brazil, is located in the semi-arid northeastern region of the country. It has historically been marked by extreme climate events, including severe droughts and sporadic floods. The inter-annual variability is highly due to the El Niño/Southern Oscillation. The annual rainfall variability is high and 75% of rainfall is expected to occur in 4 months of the year (February–May). As a result, reservoir infrastructures have been spatially distributed in the state territory to meet demands during dry months and droughts, as well as to avoid floods during extremely rainy years.

The Jaguaribe River basin occupies an area of 74,621 km^2, which is approximately 48% of Ceará State, Brazil. According to Souza Filho and Lall (2004), the main water demands are urban (20%) and irrigation (80%), which are concentrated mainly during the dry season (August–November). The water balance is negative in most months (January, February, and June through December period), when crop irrigation is most required. The study area includes the Castanhão Dam catch surface area, which supplies water for irrigated agriculture downstream, between 4°39′30″ and 4°40′00″S and 37°35′30″ and 38°27′00″W comprising 6415.10 km^2 (Fig. 1) along a 160 km-long river reach. The observed river inflow varies strongly depending on the month and the amount of rainfall. Monthly maximum values are observed in March and April (33.7 and 48.5 $m^3 s^{-1}$, respectively), and minimum values are observed in October and November (1.3 and 0.8 $m^3 s^2$, respectively). The observed annual average (1971–2000) is 13.5 $m^3 s^{-1}$. At high temperatures (averages ranging from 23 to 27 °C), irrigation occurs all year long in the target area, ranging from 3883 ha in March to a maximum of 8778 ha in August. The crop pattern varies monthly; the main crops are banana trees, rice, pasture grass, cowpea, melon, and corn, of which cowpea, melon, and corn are cultivated from July to December. A representation of 97% of the irrigated crops in the study area is shown in Table 1. This is a crop pattern update from the study by Gondim et al. (2012) after the Tabuleiro de Russas irrigation project began operational activities.

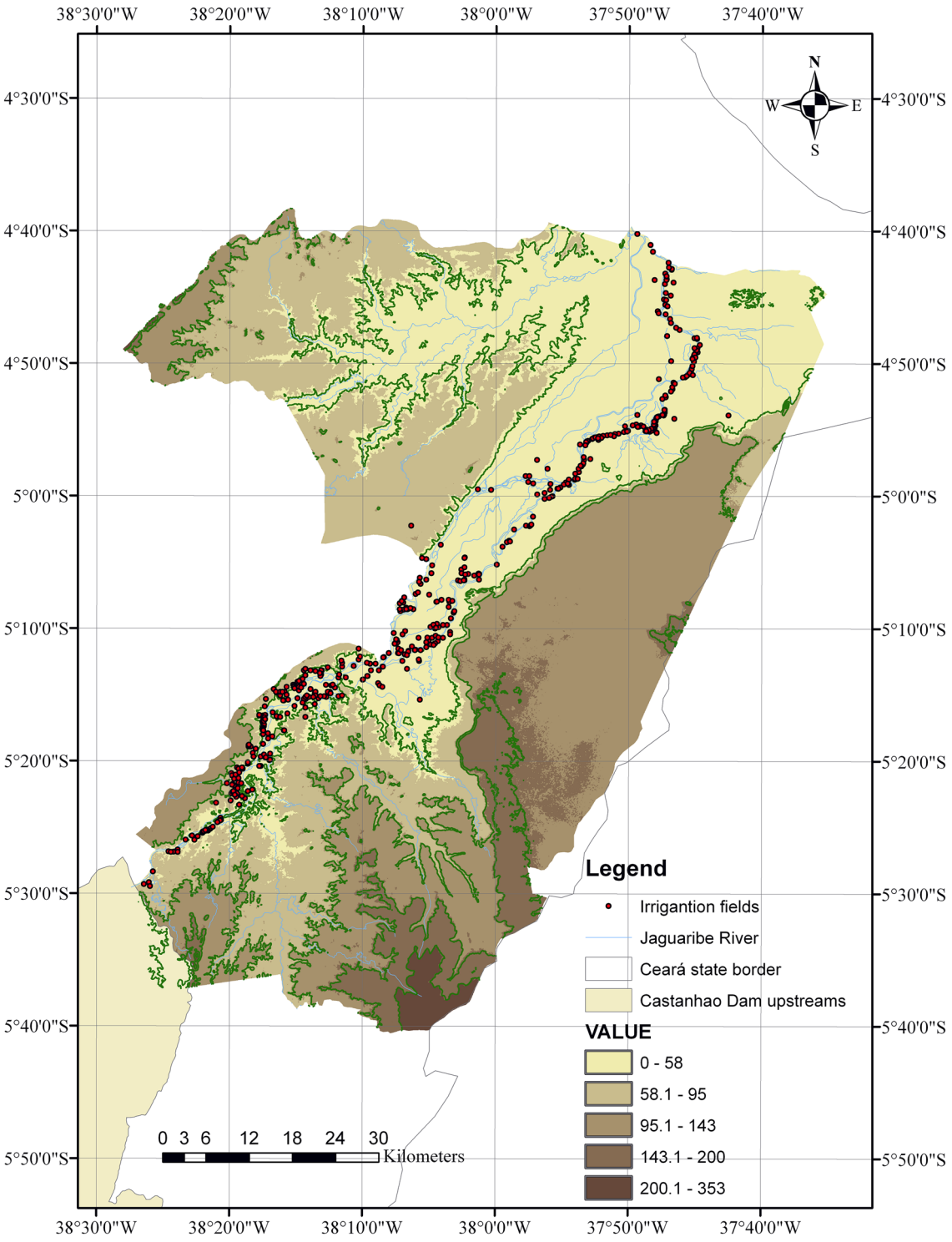

Fig. 1 Study area digital elevation model (m)

Model screening

The rainfall seasonal pattern has been used as an evaluation criterion, as it is critical to the assessment of climate change impact on water resources and agriculture. The crop growing season and river flow are dependent on the rainfall temporal distribution, and a poor seasonal representation may compromise a climate change impact assessment. In addition, it is considered that the total monthly rainfall and its seasonal occurrence obtained from GCM

Table 1 Growing months and crop areas (ha) in the study region

Crops	Jan	Feb	Mar	Apr	May	Jun	Jul	Aug	Sep	Oct	Nov	Dec
Malpighia glabra L. (acerola)	111	111	111	111	111	111	111	111	111	111	111	111
Annona sp. (soursop)	118	118		118	118	118	118	118	118	118	118	118
Gossypium hirsutum L. (cotton)								275	275	275	275	275
Anacardium occidentale L. (cashew)	44	44	44	44	44	44	44	44	44	44	44	44
Oryza sativa (rice)							1407	1407	1407	1407	1407	
Musa paradisiaca L. (banana)	2032	2041	2115	2099	2101	2153	2174	2195	2220	2195	2254	2254
Saccharum officinarum (sugar cane)	39	39	39	39	39	39	39	39	39	39	39	39
Brachiaria sp. (pasture grass)	688	686	142	142	678	678	678	722	722	722	722	722
Citrus (orange tree)	208	208	106	106	208	208	208	208	208	208	208	208
Cocos nucifera L. (coconut tree)	284	284	285	285	285	285	285	285	327	285	327	327
Vigna unguiculata (cowpea)	14	10	9	19	18	18	895	895	109	986	950	18
Papaya	17	14										
Psidium guajava (guava tree)	525	518	398	420	548	548	548	548	548	548	595	595
Mangifera indica L. (mango tree)	136	136			136	136	136	136	136	136	136	136
Citrullus vulgaris Schrad (watermelon)	138	125	82	13	5	38	132	178	175	167	132	102
Cucumis melo (melon)	306	284	232	264	262	276	363	490	480	519	501	401
Zea mays (grain) (corn)	207	220	320	511	512	512	512	834	478	437	437	115
Glycine max L. (soybean)							275	275	367	367	92	92
Pennisetum glaucum (L.) (cut grass)	18	18			18	18	18	18	18	18	18	18
Monthly irrigated area (ha)	4885	4856	3883	4171	5083	5182	7943	8778	7782	8582	8366	5575

hindcasts demonstrate a model skill to represent the present climate. Silveira et al. (2013) performed a *Seasonal Evaluation* ($EVAL_s$) of IPCC CMIP5 models for northeastern Brazil (0°S–10°S and 33°W–44°W) to identify the models that best represent twentieth century rainfall pattern. The observed data were based on an interpolated dataset from CRU and *National Oceanic and Atmospheric Administration* (NOAA). In this task, the same methodology has been applied to 25 CMIP5 models (Table 2) for Ceará State, where Jaguaribe basin is located. GCMs *Seasonal Evaluations* ($EVAL_S$) were based on the root-mean-square error (RMSE) and Pearson Correlation (CORREL.) statistics of the monthly rainfall percentage contribution relative to the annual accumulated amount, as characterized by the following equations:

$$EVAL_S = \alpha_c \frac{CORREL - CORREL_{MIN}}{CORREL_{MAX} - CORREL_{MIN}} + \alpha_r \frac{RMSE_{MAX} - RMSE}{RMSE_{MAX} - RMSE_{MIN}} \quad (1)$$

$$\alpha_c + \alpha_r = 1. \quad (2)$$

Indices α_c and α_r assume values between 0 and 1, according to the chosen CORREL and RMSE influence. In this work, 0.5 was considered to correspond to equal weights for each of the statistics. This decision may be explained by the choice to identify GCMs with equilibrium between adequate correlations with rainfall pattern in the study region and simultaneously low root-mean-square error. $EVAL_S$ assumes values between −1 and 1, ranging from perfect anti-correlation to no correlation to perfect correlation. A relative evaluation involved the minimum and maximum correlation and RMSE among models ($CORREL_{MIN}$, $CORREL_{MAX}$, $RMSE_{MIN}$, and $RMSE_{MAX}$), which allowed us to obtain the seasonal evaluation performance.

Bias removal of climate projections

The climate projections used to estimate the future water demand and availability in the Jaguaribe basin were generated by the IPCC CMIP5 GCMs for the base period of 1971–2000, as well as for 2025–2055. The choice of this future time slice is based on focusing on a near-term future to implement strategic policies for improving the sustainability of the irrigation sector and to guarantee rural employment for the next several decades. This coincides with suggestions of Taylor et al. (2009) to perform future studies when planning a CMIP5 climate change experimental design, specifically focusing on the 2026–2035 decade.

Table 2 CMIP5 GCMs $Eval_s$. Source: Sheff and Frierson (2012), Flato et al. (2013)

Model name	Institution	$EVAL_s$
CCSM4	National Center for Atmospheric Research, USA	1.000
HadGEM2-AO	National Institute of Meteorological Research/Korea Meteorological Administration	0.948
CESM1-BGC	National Science Foundation, Department of Energy, National Center for Atmospheric Research, USA	0.947
BCC-CSM1-1	Beijing Climate Center, China Meteorological Administration	0.913
GFDL-CM3	Geophysical Fluid Dynamics Laboratory, USA	0.903
CESM1-CAM5	National Science Foundation, Department of Energy, National Center for Atmospheric Research, USA	0.880
IPSL-CM5B-LR	Institut Pierre-Simon Laplace, France	0.871
GFDL-ESM2M	Geophysical Fluid Dynamics Laboratory, USA	0.845
BNU-ESM	College of Global Change and Earth System Science, Beijing Normal University	0.769
MIROC5	Atmosphere and Ocean Research Institute (The University of Tokyo), National Institute for Environmental Studies, and Japan Agency for Marine-Earth Science and Technology	0.763
INMCM4	Institute for Numerical Mathematics, RUSSIA	0.637
CSIRO-Mk3-6-0	Commonwealth Scientific and Industrial Research Organisation in collaboration with the Queensland Climate Change Centre of Excellence	0.575
GISS-E2-H	NASA Goddard Institute for Space Studies	0.566
ACCESS1-0	CSIRO (Commonwealth Scientific and Industrial Research Organisation, Australia), and BOM (Bureau of Meteorology, Australia)	0.513
IPSL-CM5A-LR	Institut Pierre-Simon Laplace, France	0.511
IPSL-CM5A-MR	CSIRO (Commonwealth Scientific and Industrial Research Organisation, Australia), and BOM (Bureau of Meteorology, Australia)	0.495
ACCESS1-3	Met Office Hadley Centre (additional HadGEM2-ES realizations contributed by Instituto Nacional de Pesquisas Espaciais)	0.487
HadGEM2-ES	Canadian Centre for Climate Modeling and Analysis	0.422
CanESM2	Japan Agency for Marine-Earth Science and Technology, Atmosphere and Ocean Research Institute (The University of Tokyo), and National Institute for Environmental Studies	0.357
MIROC-ESM	Centro Euro-Mediterraneo per I Cambiamenti Climatici, Italy	0.309
CMCC-CM	Centro Euro-Mediterraneo per I Cambiamenti Climatici, Italy	0.275
CMCC-CMS	Japan Agency for Marine-Earth Science and Technology, Atmosphere and Ocean Research Institute (The University of Tokyo), and National Institute for Environmental Studies	0.212
MIROC-ESM-CHEM	Max Planck Institute for Meteorology (MPI-M), Germany	0.188
MPI-ESM-MR	Max Planck Institute for Meteorology (MPI-M), Germany	0.040
MPI-ESM-LR	National Center for Atmospheric Research, USA	0.000

Rasmussen et al. (2012) reported a method of correcting the climate model bias by comparing the delta change (Hay et al. 2000) to distribution-based scaling (Piani et al. 2010). The conclusion was that, when using the delta change method, irrigation water demand is significantly underestimated, whereas low stream flow is overestimated. These results were due to the inability of this method to account for changes in rainfall and reference evapotranspiration interannual variability.

Statistical correction via the gamma cumulative distribution function was performed on the monthly mean precipitation time series from the IPCC-CMIP5 models using the methodology applied by Block et al. (2009). A gamma distribution was fitted to the observed monthly precipitation data (CRU) for the Castanhão Dam catchment basin to identify the probabilistic parameters that represent the monthly rainfall frequency distribution. In addition, a gamma distribution was fitted to the monthly precipitation time series obtained from the GCM *hindcasts* (from 1971 to 2000) for the basin. The GCM *hindcasts* gamma probability distribution was obtained to identify observed rainfall with the same probability, which corresponds to bias-removed present rainfall. Future rainfall bias-removed corresponds to the observed rainfall with the same probability as GCMs' future rainfall gamma distribution. Considering the lack of a historical temperature measurement data set, minimum and maximum temperatures from IPCC-CMIP5 GCMs were statistically corrected using temperature data from CRU (Harris et al. 2014), which is defined by the following equation:

$$t'_{\mathrm{p}} = \frac{t_{\mathrm{p}} - \bar{t}_{\mathrm{h}}}{\mathrm{std}_{\mathrm{th}}} \mathrm{std}_{\mathrm{obs_t}} + \bar{t}_{\mathrm{obs}}, \tag{3}$$

where t'_p is the minimum or maximum mean monthly temperature bias-removed; t_p is the monthly minimum or maximum mean monthly temperature from the GCM projection (2025–2055) time slice to be corrected; $\bar{t}_h$ is the minimum or maximum mean monthly temperature from the GCM *hindcasts* (1971–2000) time slice; std_{th} is the standard deviation of the minimum temperature or maximum temperature from the GCM *hindcasts* (1971–2000) time slice; std_{obs_t} is the standard deviation of the minimum temperature or maximum temperature from the CRU (1971–2000) time slice; $\bar{t}_{obs}$ is the minimum or maximum mean temperature from the CRU (1971–2000) time slice.

The IPCC fifth report introduced the concept of effective radioactive forcing (anthropogenic plus natural), measured in W m^{-2} (Myhre et al. 2013). Four future emission scenarios called *Representative Concentration Pathways* (RCPs) (RCP2.6; RCP4.5; RCP6.0; RCP8.5) were developed. In addition to the scenarios designed in the *Special Report on Emission Scenarios* (SREs) (Nakicenovic et al. 2000), in the third and fourth reports, these four scenarios also include a more consistent approach to short life gases, land-use change, and radioactive driving force stabilization by 2100 (low 2.6 W m^{-2}, medium–low 4.5 W m^{-2}, and medium–high 6.0 W m^{-2} or high 8.5 W m^{-2}) (Cubasch et al. 2013).

Estimating Castanhão Dam water inflow

Present and future water availability in the Jaguaribe basin was estimated using the *Soil Moisture Accounting Procedure* (SMAP) rainfall—river flow hydrological model and bias-removed rainfall as the input climate data set. The SMAP model was calibrated against monthly stream flow from 1912 to 1969. The correlation coefficient (CORREL.) between observed and modeled values was 0.90. Validation was performed over the 1974–1996 period (CORREL. = 0.95), indicating a very strong model performance. The SMAP model runs a monthly time step containing two reservoirs (subsurface and groundwater) and four parameters (*soil saturation capacity; subsurface flow; recharge coefficient; a base flow recession coefficient*), which makes it appropriate for application to big basins (Block et al. 2009).

Estimating reference evapotranspiration

According to Allen et al. (1998), crop evapotranspiration (ET_c) refers to the evaporation demand for crops that are grown under optimal soil water, excellent management, and environmental conditions, and that achieve full production under the given climate. ET_c depends on the reference evapotranspiration (ET_o) and crop development stage measured by the crop coefficient (Kc). Crop water needs (CWN) are equal to crop evapotranspiration, also called the net irrigation requirements (NIR). Irrigation systems provide water to crops, but part of this water is lost by evaporation, run-off or leaching. Silva et al. (2007) applied the irrigation water needs (IWN) term, hereinafter referred to as the amount of water to meet ET_c plus expected water losses by irrigation, which may be associated with irrigation system technology and its operational and management procedures. Bias-removed maximum and minimum temperatures from IPCC-AR5 GCMs were applied to estimate reference evapotranspiration, using the limited climate data model by Penman–Monteith (Allen et al. 1998). The evaluation and processing steps to assess water demand and availability are represented in Fig. 2. The complete mathematical model by FAO-Penman–Monteith (Allen et al. 1998) requires a complete data set of climate variables from a reference station to estimate reference evapotranspiration, which is given by the following equation:

$$ET_o = \frac{0.408\Delta(Rn - G) + \gamma \frac{900}{T+273} u_2 (e_s - e_a)}{\Delta + \gamma(1 + 0.34u_2)}, \quad (4)$$

where ET_o is the reference evapotranspiration (mm day^{-1}); Rn is the net radiation at the crop surface (MJ m^2 day^{-1}); G is the soil heat flux density (MJ m^2 day^{-1}); T is the average daily air temperature measured at a height of 2 m (°C); u_2 is the wind speed at a height of 2 m (m s^{-1}); e_s is the saturation vapor pressure (kPa); e_a is the actual vapor pressure (kPa); $e_s - e_a$ is the saturation vapor pressure deficit (kPa); Δ is the slope of the vapor pressure curve (kPa $°C^{-1}$); γ is the psychometric constant (kPa $°C^{-1}$).

The meteorological data required to estimate the Penman–Monteith ET_o consist of air temperature, air humidity, wind speed, and radiation. A climate data set containing maximum and minimum temperatures, actual and saturation vapor pressures, liquid radiation, and wind speed allows for the estimation of the Penman–Monteith FAO ET_o by applying a source of equations, the so-called limited climatic data model procedure suggested by Allen et al. (1998). Popova et al. (2006) in Bulgaria, Jabloun and Sahli (2008) in Tunisia, and Sentelhas et al. (2010) in Canada have validated this model for each of the sites. For the study region, the validation procedure has been done by Gondim et al. (2012).

Estimating irrigation water needs (IWN)

The irrigation water needs (IWN) (Eq. 5) in the basin were estimated using the approach applied by Gondim et al. (2012), where weighted crop coefficient (WKc) estimations for the irrigated crops in each particular month (Table 1) were obtained by multiplying each Kc (Table 3) by the respective crop area divided by the total monthly irrigated area. The meaning of WKc is the evaporation

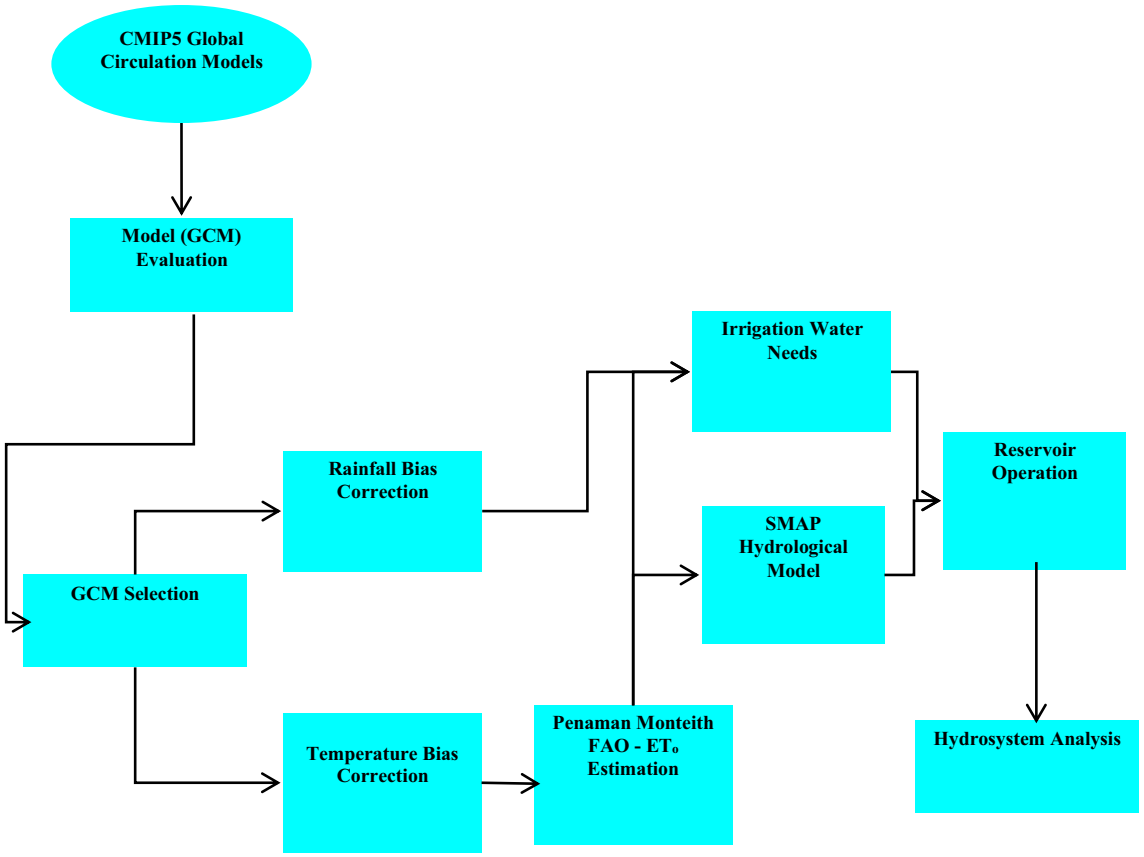

Fig. 2 *Coupled Model Intercomparison Project Phase 5* (CMIP5) Global Circulation Models (GCMs) evaluation criteria and processing to assess water demand and availability. ET_o, reference evapotranspiration; SMAP, *Soil Moisture Accounting Procedure*

demand coefficient of a *basket* of crops weighted by the area to be used to estimate all crop evapotranspiration by month. The weighted monthly irrigation efficiency (WEf) (Table 4) was calculated similarly, using the average field measured efficiency (Ef as obtained by field evaluation) for each irrigation system adopted by farmers, multiplied by the area of each irrigation system, and then divided by the total irrigated area of each month, as shown in Table 4. Thus, WEf refers to the weighted-average Ef of all systems in operation by month. The area occupied by each crop varied each month, as did the irrigation systems, which resulted in different monthly WKc and WEf values:

$$\mathrm{IWN} = \frac{\mathrm{ET_o} \cdot \mathrm{WKc}_i}{\mathrm{WEf}_i} - P_i \tag{5}$$

where ET_o is the Penman–Monteith FAO reference evapotranspiration (mm month^{-1}); WKc_i is the weighted crop coefficient for month i (dimensionless); WEf_i is the weighted irrigation efficiency for month i (dimensionless); P_i is the average monthly effective rainfall for month i (mm).

The four factors for projected climate and hydrological variables in the RCP4.5 and RCP8.5 scenarios are (1) rainfall (mm), (2) reference evapotranspiration (mm) estimated from minimum and maximum temperature (°C) by the Penman–Monteith limited data model (Allen et al. 1998), (3) irrigation water needs (IWN, mm), and (4) river flow (Q, m^3 s^{-1}). CRU represents measured climate data. Maximum and minimum temperature and rainfall bias-removed input data (Table 5) were obtained from GCM hindcasts and model future projections output. Climate change impact analysis was based on anomalies, which were calculated by the difference between the twenty-first and twentieth century time slice annual averages, divided by the twentieth century annual average. Anomalies may then assume negative or positive values (signs). When GCM future projections of a certain climate variable disagree, this disagreement may be attributed to uncertainties surrounding modeling the future climate. According to Cubasch et al. (2013), model uncertainty is an important contributor to discrepancies in climate predictions and projections. Some use this term to represent the range of behaviors observed in ensembles of climate models (model spread). Causes of this range may be the uncertainty in greenhouse gas future emissions (scenarios), the model

Table 3 Crop coefficients (Kcs) of each growing crop by month and respective monthly weighted Kc

Crop	Jan	Feb	Mar	Apr	May	June	July	Aug	Sep	Oct	Nov	Dec
Malpighia glabra L. (acerola)	1.39	1.39	1.39	1.39	1.39	1.39	1.39	1.39	1.39	1.39	1.39	1.39
Gossypium hirsutum L. (cotton)								0.50	1.05	1.05	1.05	0.70
Annona sp. (soursop)	0.95	0.95	0.95	0.95	0.95	0.95	0.95	0.95	0.95	0.95	0.95	0.95
Cashew	0.55	0.55	0.55	0.55	0.55	0.55	0.55	0.55	0.55	0.55	0.55	0.55
Oryza sativa (rice)							1.05	1.20	0.90	0.90	0.90	0.90
Musa paradisiaca L. (banana)	1.10	1.10	1.10	1.10	1.10	1.10	1.10	1.10	1.10	1.10	1.10	1.10
Saccharum officinarum (sugar cane)	1.25	1.25	1.25	1.25	1.25	1.25	1.25	1.25	1.25	1.25	1.25	1.25
Brachiaria sp. (pasture grass)	0.75	0.75	0.75	0.75	0.75	0.75	0.75	0.75	0.75	0.75	0.75	0.75
Citrus (orange tree)	0.85	0.85	0.85	0.85	0.85	0.85	0.85	0.85	0.85	0.85	0.85	0.85
Cocos nucifera L. (coconut tree)	1.00	1.00	1.00	1.00	1.00	1.00	1.00	1.00	1.00	1.00	1.00	1.00
Vigna unguiculata (cowpea)	0.75	1.2	0.75	1.2	0.75	1.2	0.75	1.2	0.75	1.2	0.75	1.2
Papaya	0.91	0.91										
Psidium guajava (guava tree)	0.63	0.63	0.63	0.63	0.63	0.63	0.63	0.63	0.63	0.63	0.63	0.63
Mangifera indica L. (mango tree)	0.71	0.71	0.71	0.71	0.71	0.71	0.71	0.71	0.71	0.71	0.71	0.71
Citrullus vulgaris Schrad (watermelon)	0.41	1.36	0.71	0.41	1.36	0.71	0.41	1.36	0.71	0.41	1.36	0.71
Cucumis melo (melon)	0.21	1.21	0.98	0.21	1.21	0.98	0.21	1.21	0.98	0.21	1.21	0.98
Zea mays (grain) (corn)	0.49	1.06	0.95	0.95	0.49	1.06	0.95	0.95	0.49	1.06	0.95	0.95
Glycine max L. (soybean)	0.71	1.71	1.00	0.80	0.71	1.71	1.00	0.80	0.71	1.71	1.00	0.80
Pennisetum glaucum (L.) (cut grass)	0.75	0.75	0.75	0.75	0.75	0.75	0.75	0.75	0.75	0.75	0.75	0.75
Monthly weighted Kc	0.87	0.97	1.00	0.95	0.92	0.96	0.91	0.99	0.84	0.97	0.89	0.92

Crop coefficient (Kc): evaporating demand coefficient from each crop used to estimate crop evapotranspiration (ETc). Monthly weighted Kc: evaporating demand coefficient of a *basket* of crops weighted by each crop area to be used to estimate all crops evapotranspiration by month

Table 4 Total area of irrigation systems type in operation each month and respective irrigation field efficiency (Ef), monthly weighted efficiency (WEf), and monthly improved (WEf)

Irrigation systems (ha)	Ef	Improved Ef	Jan	Feb	Mar	Apr	May	Jun	Jul	Aug	Sep	Oct	Nov	Dec
Paddy rice and level basing	0.52	0.58	392	392	110	110	392	392	1853	1861	1797	1861	1861	394
Furrow	0.54	0.60	176	176	63	69	176	176	317	333	201	333	330	178
Sprinkler	0.64	0.71	63	63	12	12	63	63	572	591	82	591	589	64
Microsprinkler and drip	0.74	0.85	3587	3552	3174	3241	3712	3604	4111	3955	3681	3953	4076	3935
Pivot	0.65	0.72	667	673	524	739	740	947	1090	2038	2021	1844	1510	1004
Total irrigated area			4885	4856	3883	4171	5083	5182	7943	8778	7782	8582	8366	5575
Monthly WEf			0.70	0.70	0.72	0.71	0.70	0.70	0.66	0.66	0.66	0.66	0.60	0.70
Monthly improved WEf			0.80	0.80	0.82	0.82	0.80	0.80	0.75	0.74	0.75	0.74	0.75	0.80

Total area of irrigation systems type in operation each month refers to the area of irrigation systems being used by method of water application each month

Ef actual irrigation efficiency performance achieved in the field by a certain system, *WEf* average Ef of all systems being operated in each month weighted by each system area, *improved WEf* average of desirable irrigation efficiency performance achieved in the field by a certain system weighted by each system area by month

uncertainty used to represent climate, internal climate variability, modeling drivers forcing, and the initial and boundary conditions used in model runs.

In addition, an irrigation water demand scenario was run by applying improved irrigation efficiency (Table 4), along with possible gains by irrigation system management performance, based on each irrigation system with adopted technology.

Climate change impacts were quantified by comparing the present climate and hydrological variables (1971–2000) to future projections (2025–2055 time slices) for the RCP4.5 and RCP8.5 scenarios. GCMs that

Table 5 Mean climate variable input data (bias-removed)

CRU/models	1971–2000 BASELINE			2025–2055 RCP4.5			2025–2055 RCP4.5		
	T_{min} (°C)	T_{max} (°C)	Rainfall (mm year^{-1})	T_{min} (°C)	T_{max} (°C)	Rainfall (mm year^{-1})	T_{min} (°C)	T_{max} (°C)	Rainfall (mm year^{-1})
CRU	21.0	32.0	781	–	–	–	–	–	–
CCSM4	23.4	30.4	950	24.9	31.9	804	25.1	32.0	930
HadGEM2-AO	22.1	30.0	948	24.4	31.2	868	24.1	31.2	840
CESM1-BGC	23.5	31.3	949	25.3	32.2	835	24.2	32.2	866
BCC-CSM1.1	23.0	29.8	949	24.3	31.7	995	25.5	33.1	856
GFDL-CM3	23.2	29.7	944	24.8	32.7	1,062	24.6	33.5	928

HadGEM2-AO Hadley Centre New Global Environmental Model 2-Arctic Oscillation, *CESM1-BGC* Community Earth System Model 1-Biogeochemical, *GFDL-CM3* Geophysical Fluid Dynamics Laboratory-Coupled Model 3, *CRU* Climate Research Unit, *CCSM4* Community Earth System Model 4, *BCC.CSM1.1* Beijing Climate Center-Climate System Model 1.1

presented the five highest scored $EVAL_S$ were selected for evaluation by this impact assessment.

Estimating future water shortage

The annual water-deficit index (I) is defined as a performance indicator using annual water availability (S) and irrigation water demand (D) as follows:

$$I = \frac{S - D}{D}, \tag{6}$$

where S is the total annual water storage (m^3) and D is the total irrigation water demand (m^3). $I \geq 0$ indicates that no water-deficit exists. A lower I value indicates less water availability. $I \leq 0$ indicates agricultural water deficit (Moursi et al. 2017).

Results

Seasonal evaluation

For the $EVAL_s$, Fig. 3 shows a three-dimensional representation of the results for RMSE (X-axis), $EVAL_s$ (Y-axis), and CORREL (Z-axis). Models with high RMSE and low CORREL are located to the right of the X-axis and at the bottom of the Z-axis. Models shown in blue have high CORREL and low RMSE, and are located to the left of the X-axis at the top of Fig. 3, as a consequence of having high EVALs. Five GCMs exhibited $EVAL_s$ indices above 0.90, which were the *Community Earth System Model 4* (CCSM4), *Hadley Centre New Global Environmental Model 2-Arctic Oscillation* (HadGEM2-AO), *Community Earth System Model 1-Biogeochemical* (CESM1-BGC), *Beijing Climate Center-Climate System Model* 1.1 (BCC-CSM1.1), and *Geophysical Fluid Dynamics Laboratory-Coupled Model 3* (GFDL-CM3), which presented $EVAL_S$ of 1.000, 0.948, 0.947, 0.913, and 0.903, respectively. This result suggests that these models

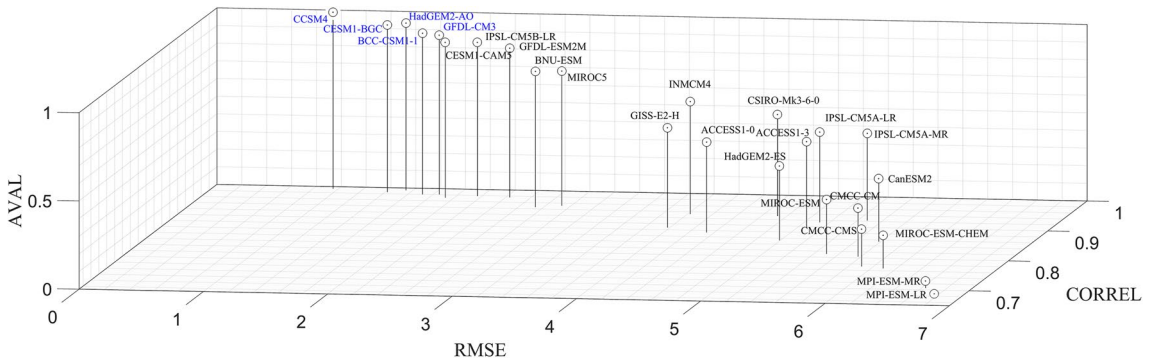

Fig. 3 CMIP5 GCMs' EVALs for Ceará State, Northeast of Brazil

are appropriate CMIP5 GCMs for running hydrological studies on the rainfall output dataset for Ceará State.

Among all 25 CMIP5 models used for the study region, the five mentioned GCMs performed the best for rainfall pattern. This GCM screening criterion may be more appropriate for application to the previous hydrological studies, because future projections for rainfall are more uncertain than those for temperature. Model selection was based on the assumption that the models should be able to run more likely future projections, and anomaly sign disagreement was smoothed by bias-removing techniques using the cumulative gamma distribution function. Models selected for future climate data were submitted to bias correction, excluding model over- and underestimation values, compared to the observed data.

Climate variable projections

All five selected CMIP5 models projected future temperature increases (positive sign) for both the RCP4.5 scenario and the RCP8.5 scenario (Fig. 4). The observed differences among the models are related to the magnitude of the change, showing positive sign anomalies in all months of the year. Figure 5 provides both reference evapotranspiration and rainfall changes for the five selected CMIP5 models.

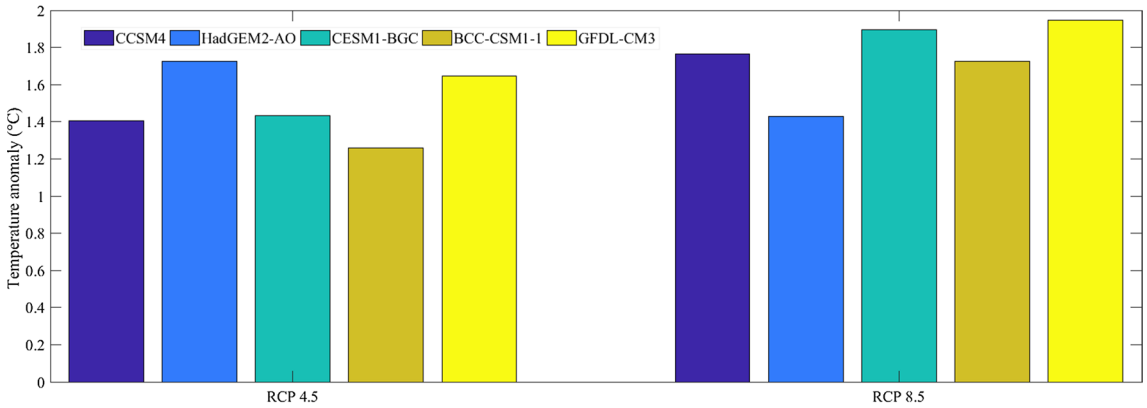

Fig. 4 Temperature anomaly

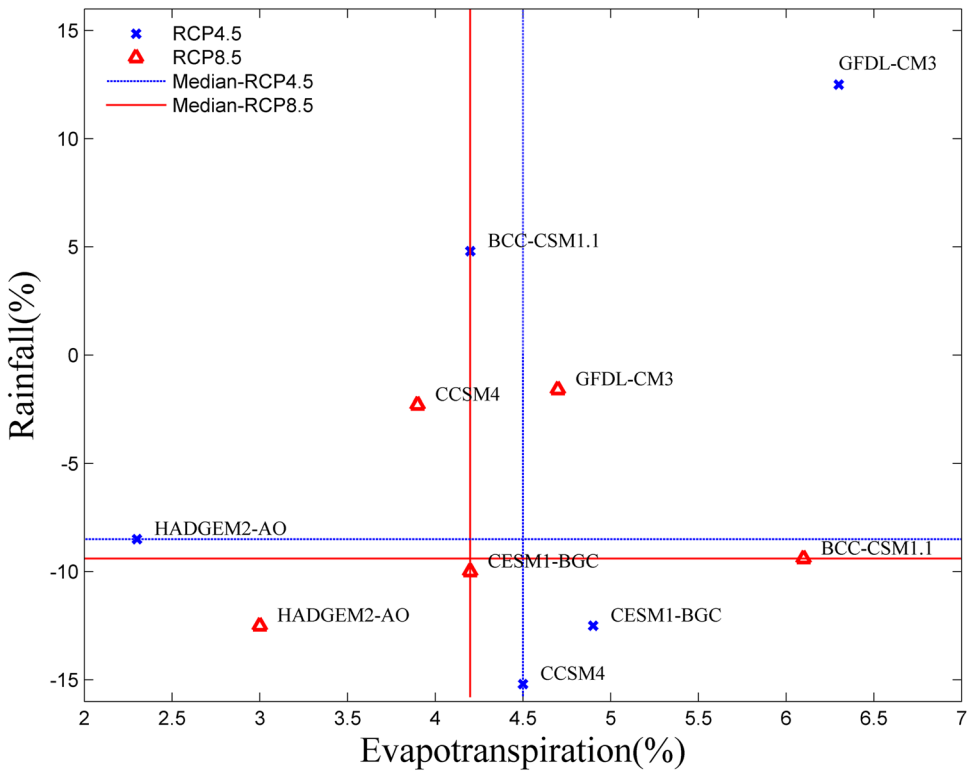

Fig. 5 Rainfall and evapotranspiration anomaly (%)

Due to higher temperatures occurring in the future, the five selected GCMs projected only positive change signs for ET_o, with average increases ranging from 2.3 to 6.3% for the 2025–2055 time slice relative to the 1971–2000 baseline period (scenarios RCP4.5 and RCP8.5). This percentage represents annual ET_o increases ranging from 42 to 112 mm. In regard to rainfall, uncertainties still remain surrounding the projections of the CMIP5 models, as positive and negative anomalies (%) were observed in the RCP4.5 scenario and only negative anomalies were observed in the RCP8.5 scenario (Fig. 5). In other words, differences exist in the sign change depending on the model, scenario, and month of the year. Three of the five models (CCSM4, HADGEM2-AO, and CESM1-BGC) projected annual decreases (from −8.5 to −15.2%), and two models (BCC-CSM1.1 and GDFL-CM3) projected increases (varying from 4.8 to 12.5%) (RCP4.5 scenario). All five selected GCMs projected decreases (varying from −1.6 to −12.5%) (RCP8.5 scenario), as observed in Fig. 5. The changes represent decreases ranging from 81 to 144 mm annually or increases from 46 to 118 mm (RCP4.5). The RCP8.5 scenario showed decreases ranging from 17 to 139 mm annually.

Future water availability and demand

The sign changes of the annual river inflow (%) into Castanhão Dam follow rainfall behavior uncertainties, varying by GCM and by scenario, as represented in Fig. 6. The HadGEM-AO and CESM1-BGC models projected that annual river run-off would become lower in both scenarios (−43.7 and −50.3%) for RCP4.5 and (−43.4 and −26.8%) for RCP8.5. The CCSM4, BCC-CSM1.1, and GDFL-CM3 models projected values of −48.9, 19.8, and 3.5%, respectively, for RCP4.5 and of 3.8, −43.0, and −8.4%, respectively, for RCP8.5. Most scenarios projected future reductions; this lower water availability should be taken into consideration in future policy adaptation and strategy design.

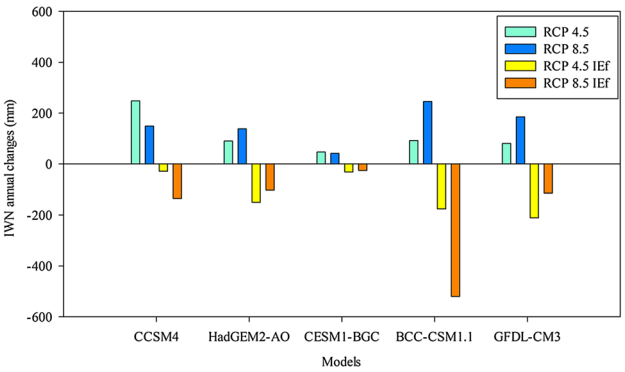

Fig. 7 IWN anomaly (mm) by model, scenario, and improved irrigation efficiency (IEF)

Projected increases in ET_o and rainfall anomalies resulted in greater annual IWN for the 2025–2055 future time slice for all five models and applied scenarios. Average annual increases ranged from 3.1 to 16.7% (RCP4.5 scenario) and from 2.8 to 16.7% (RCP8.5 scenario), representing a 42–248 mm irrigation water demand annually (Fig. 7). When applying an improved irrigation efficiency scenario, water availability could meet irrigated agriculture demand (IWN) (Fig. 7) according to all five GCMs (RCP4.5 scenario and RCP8.5 scenario) if greater irrigation system efficiencies (IEf) are reached (Table 4) in the river basin. Annual water demand changes varied from −1.9 to −14.7% (RCP4.5), and from −1.7 to −35.2% (RCP8.5), representing a −29 to −211 mm and −26 to −520 mm annual demand, respectively.

Lower future water availability is projected, as detected by less positive water-deficit index (*I*) in all models except for the BCC-CSM1.1 and GDFL-CM3 models in the

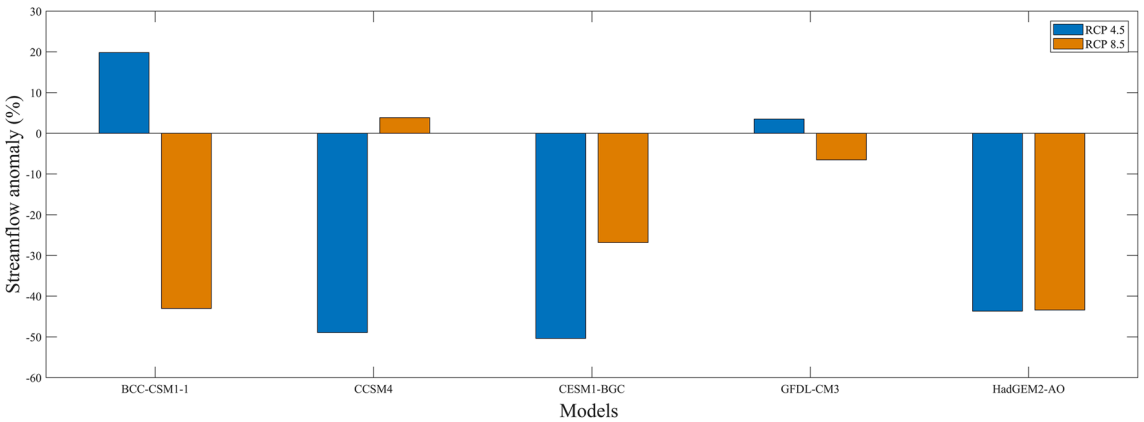

Fig. 6 Streamflow anomaly (%)

RCP4.5 scenario and by all models in the RCP8.5 scenario. No water deficit is projected ($I > 0$) when only agriculture water is studied (Fig. 8).

Discussion of results

Woznicki et al. (2015) applied ten bias-removed GCMs to conclude that the Kalamazoo, Michigan basin water balance depended strongly on the sign and magnitude of the rainfall and temperature obtained from the GCMs. They also reported uncertainties about the future, and recommended that the sign and magnitude of the rainfall and temperature obtained from the GCMs should be considered in water resource storage and supply. Even though this task has been developed only with the selected rainfall seasonally evaluated GCMs, uncertainties about future projected rainfall and, consequently, basin water balance still persist.

The magnitude of the IWN change was not great enough to cause a collapse in water supply considering agriculture demand only, unless it was associated with food demand and irrigated area increases. In this case, an adaptation policy should be implemented to achieve a sustainable water supply to meet demands.

Improved irrigation water use efficiency (IEf) (Fig. 7) has been demonstrated to play an important role in adaptation to future higher levels of irrigation water demand. Elliot et al. (2014) also reported that efforts to increase water use efficiency could compensate for climate change without further exploiting water resources in rivers due to water loss reduction. Similar conclusions were reported by Panagoulia (2004) in Greece. Therefore, adaptation measures should be applied to irrigation water use efficiency improvement at the field level to adopt water use technologies and for improvement of water resource management. System operation, delivery of precisely estimated quantities of water as needed by users, and installation of water meters should be considered. As reported by Rehana and Mumjumdar (2013), assessment studies on climate change impacts on irrigation demand should help in developing adaptation policies for reservoir operations.

Despite the future increase in rainfall projected by some GCMs, they are not enough to compensate for water demand increases for irrigation due to the higher projection of ET_o. This occurs, because the rainfall increase is mostly observed in the rainy season, whereas irrigation demand mostly occurs in the second semester of the year. The availability of water supply when needed shows a dependence on storage infrastructure and efficient management. Ashofteh et al. (2013) also projected increases in water demand for irrigation (16%) using the HadCM3 model for both positive and negative rainfall projection signs for the Aidoghmoush River, Azerbaijan. Mainuddin et al. (2015) also reported increases in irrigation water demand using two models with different rainfall signs in Bangladesh. A similar situation was reported by Zamani et al. (2016) in a study on the effects of climate change on agricultural water requirements in Iran. Regular changes and increases in temperature and an irregular change in precipitation (either decreasing or increasing) were expected in the future compared to the base period. Increases in the amount of the net water requirement and water demand volume for irrigation were projected in the future, as well.

To provide a precise time for and quantity of irrigation, efficient water use strategies should also focus on meteorological station availability for ET_o estimation, Kc (determined by crop and development stage), adoption of soil water retention practices and dissemination of technical information to farmers.

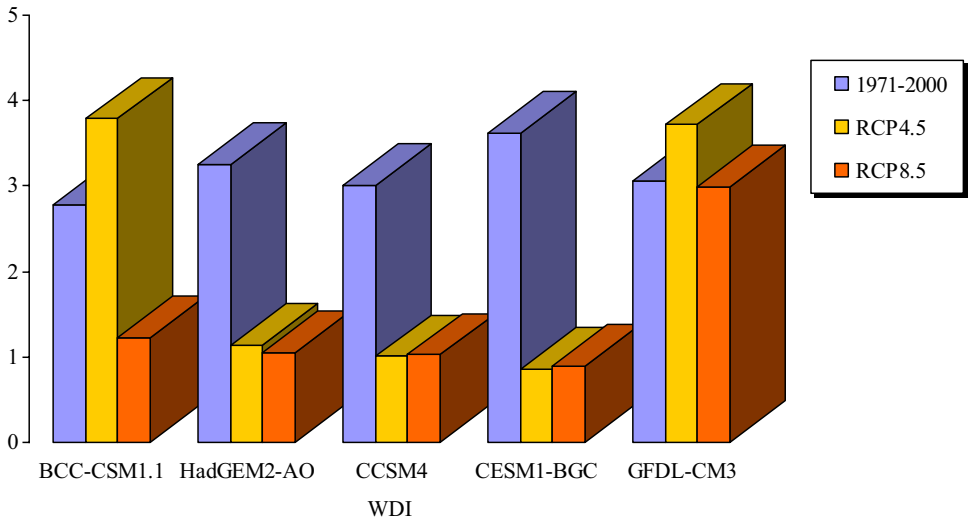

Fig. 8 Water-deficit index by model (1971–2000) and (2025–2055), RCP4.5 and RCP8.5

The most important source of water demand increases to consider in the Jaguaribe River basin is the expansion of monthly irrigated fields, which may be observed by comparing the maximum of 5957 ha in October, as reported by Gondim et al. (2012), and now 8778 ha in August. Mainuddin et al. (2015) also reported that the increasing water demand for irrigation due to climate change may be less significant than the impact of food demand increases, which are drivers for irrigated crop area expansion.

Aside from climate change, water supply capacity assessment of the Castanhão Dam should address key points such as other water use sectors, irrigated agricultural expansion regulations limited to water availability, identification of possible reservoir system operation failures to meet demand, and adaptation measures to prepare farmers for future challenges. This should include the need to share water resources and avoid conflicts between users. Other water use sectors should be included in future studies to analyze water sustainability and continuation of the current agriculture water use behavior may no longer be sustainable.

Conclusion

Five climate change models were selected by rainfall seasonal evaluation performance criteria. These models were used to run a climate change impact assessment on irrigation water availability and demand. Climate change is projected to increase temperature and reference evapotranspiration and thus water resource demand for irrigated agriculture in the studied basin, according to all five selected CMIP5 GCMs.

Even though CMIP5 has brought about improved GCMs, climate models still disagree on future projections for rainfall, as observed in the different signs of future changes. Uncertainties in the future climate will persist until models are improved and there is a better understanding of the greenhouse gas response to climate change, especially to rainfall compared to future temperature.

It has been demonstrated that even in cases where rainfall has a positive sign, the increased magnitude is not sufficient to compensate for water demand increases caused by higher ET_o. This may be because these observed rainfall increases are expected to occur during the rainy season, which does not relieve increasing demand in the second semester (dry season) of each year.

Uncertainties were also observed in average river flow, as positive and negative sign anomalies were projected by different models and scenarios. Most scenarios project future decreases, which implies less water storage and availability.

When assessing the future climate in addition to the irrigation area expansion in the basin, it is expected that available water will become even scarcer. Comparing the water demand increase caused by rainfall and ET_o magnitude change to the irrigated area expansion, the latter is a relevant driver of water stress.

If current practices persist, the available water may not meet future irrigation demands. Sustainable water strategies should address climate change and food demand increase scenarios; water scarcity is the main challenge for the agriculture sector and water managers in semi-arid regions. Sustainability of irrigated agriculture is at risk in the Jaguaribe River basin, and climate change can be a negative influence.

It is possible to reduce future water demand and to compensate for demand increases caused by climate change by achieving improved irrigation water use efficiency, as demonstrated by all models and the output of the studied scenarios.

Even though the water-deficit index (I) is positive, when only agriculture water is considered, I is expected to become lower in the future, indicating a lower water availability for agriculture.

Future studies to identify critical failures in water supply for irrigation and reservoir-stored water availability should consider other water use sectors for delineating policy aimed at water regulatory rules to prioritize access by category users.

Acknowledgements The authors would like to thank the Brazilian Corporation for Agriculture Research—Embrapa (Grant no. MP1 01.12.01.001.05.00) and National Research Council—CNPq (Grant no. Adapta MCTI/CNPq/ANA N ° 23/2015).

References

Allen RK, Pereira LS, Raes D, Smith M (1998) Crop evapotranspiration. Guideline for computing crop water requirements. FAO irrigation and drainage paper no. 56. United Nations Food and Agricultural Organization, Rome

Ashofteh PS, Haddad OB, Mariño MA (2013) Climate change impact on reservoir performance indexes in agricultural water supply. J Irrig Drain 139:85–97

Barbieri AF, Domingues E, Queiroz BL, Ruiz RM, Rigoti JI, Carvalho JAM, Resende MF (2010) Climate change and population migration in Brazil's Northeast: scenarios for 2025–2050. Popul Environ 31:344–370. https://doi.org/10.1007/s11111-010-0105-1

Block PJ, Souza Filho FA, Sun L, Kwon H-H (2009) A streamflow forecasting framework using multiple climate and hydrological models. J Am Water Resour Assoc 45:828–843. https://doi.org/10.1111/j.1752-1688.2009.00327.x

Cubasch UD, Wuebbles D, Chen MC, Facchini D, Frame N, Mahowald J-G, Winther (2013) Introduction. In: Stocker TF, Qin D, Plattner G-K, Tignor M, Allen SK, Boschung J, Nauels A, Xia Y, Bex V, Midgley PM (eds.) Climate change (2013) the physical science basis. Contribution of Working Group I to the fifth assessment report of the intergovernmental panel on climate change. Cambridge University Press, Cambridge

Elliot J, Deryng G, Müller C et al (2014) Constraints and potentials of future irrigation water availability on agricultural production under climate change. Proc Natl Acad Sci USA 111:3239–3244. https://doi.org/10.1073/pnas.1222474110

Flato GJ, Marotzke B, Abiodun P, Braconnot SC, Chou W, Collins P, Cox F, Driouech S, Emori V, Eyring C, Forest P, Gleckler E, Guilyardi C, Jakob V, Kattsov C, Reason M, Rummukainen (2013) Evaluation of climate models. In: Stocker TF, Qin D, Plattner G-K, Tignor M, Allen SK, Boschung J, Nauels A, Xia Y, Bex V, Midgley PM (eds.) Climate change (2013) the physical science basis. Contribution of Working Group I to the fifth assessment report of the intergovernmental panel on climate change. Cambridge University Press, Cambridge

Gondim RS, Castro MAH de, Maia A, de HN, Evangelista, Fuck SRM, de SC F.J (2012) Climate change impacts on irrigation water needs in the Jaguaribe River Basin1. J Am Water Resour Assoc 48:355–365. https://doi.org/10.1111/j.1752-1688.2011.00620.x

Harris I, Jones PD, Osborn TJ, Lister DH (2014) Updated high-resolution grids of monthly climatic observations—the CRU TS3.10 dataset. Int J Climatol 34:623–642. https://doi.org/10.1002/joc.3711

Hay LE, Wilby RL, Leavesley GH (2000) A comparison of delta change and downscaled GCM scenarios for three mountainous basins in the United States. J Am Water Resour Assoc 36:387–397. https://doi.org/10.1111/j.1752-1688.2000.tb04276.x

Hong EM, Namc WH, Choid JY, Pachepsky YA (2016) Projected irrigation requirements for upland crops using soil moisture model under climate change in South Korea. Agric Water Manag 165:163–180. https://doi.org/10.1016/j.agwat.2015.12.003

Jabloun M, Sahli A (2008) Evaluation of FAO-56 methodology for estimating reference evapotranspiration using limited climatic data application to Tunisia. Agric Water Manag 95:707–715. https://doi.org/10.1016/j.agwat.2008.01.009

Krol MS, Bronstert A (2007) Regional integrated modeling of climate change impacts on natural resources and resources usage in semi-arid Northeast Brazil. Environ Model Softw 22:259–268. https://doi.org/10.1016/j.envsoft.2005.07.022

Maeda EE, Pellikka PKE, Clark BJF, Siljander M (2011) Prospective changes in irrigation water requirements caused by agricultural expansion and climate changes in the eastern arc mountains of Kenya. J Environ Manag. https://doi.org/10.1016/j.jenvman.2010.11.005

Mainuddin M, Kirby M, Chowdhurry RAR, Shah-Newaz SM (2015) Spatial and temporal variations of, and the impact of climate change on, the dry season crop irrigation requirements in Bangladesh. Irrig Sci 33:107–120. https://doi.org/10.1007/s00271-014-0451-3

Moursi H, Kim D, Kaluarachchi J (2017) A probabilistic assessment of agricultural water scarcity in a semi-arid and snowmelt-denominated river basin under climate change. Agric Water Manag 193:142–152. https://doi.org/10.1016/j.agwat.2017.08.010

Myhre GD, Shindell F-M, Bréon W, Collins J, Fuglestvedt J, Huang D, Koch J-F, Lamarque D, Lee B, Mendoza T, Nakajima A, Robock G, Stephens T, Takemura H, Zhang (2013) Anthropogenic and natural radiative forcing. In: Stocker TF, Qin D, Plattner G-K, Tignor M, Allen SK, Boschung J, Nauels A, Xia Y, Bex V, Midgley PM (eds.) Climate change 2013: the physical science basis. Contribution of Working Group I to the fifth assessment report of the intergovernmental panel on climate change. Cambridge University Press, Cambridge

Nakicenovic N, Alcamo J, Davis G, De Vries B, Fenhann J, Gaffin S, Gregory K, GR A, Jung TY, Kram T, LaRovere EL, Michaelis L, Mori S, Morita T, Pepper W, Pitcher H, Price L, Riahi K, Roehrl A, Rogner HH, Sankovski A, Schlesinger M, Shukla P, Smith S, Swart R, Van Rooijen S, Victor N, Dadi Z, (2000) IPCC special report on emission scenarios. In: Nakicenovic N, Swart R (eds). Cambridge University Press, Netherlands

Panagoulia D (2004) Climate change effects on spatial distribution of Thessaly Plain irrigation, Greece. Geophys Res Abstrs 6:25–30. https://doi.org/10.13140/2.1.1155.5523

Panagoulia D, Bili H (2002) Climate change effects on spatial distribution of cotton irrigation in Thessaly Plain of Greece. http://users.itia.ntua.gr/dpanag/d19.pdf. Accessed 11 Jul 2017

Piani C, Haerter JO, Coppola E (2010) Statistical bias correction for daily precipitation in regional climate models over Europe. Theor Appl Climatol 99:187–192. https://doi.org/10.1007/S00704-009-0134-9

Popova Z, Kercheva M, Pereira LS (2006) Validation of the FAO methodology for computing ET_o with limited data. Application to South Bulgaria. J Irrig Drain 55:201–215. https://doi.org/10.1002/ird.228

Rasmussen J, Sonnenborg TO, Stisen S, Seaby LP, Christensen BSB, Hinsby K (2012) Climate change effects on irrigation demands and minimum stream discharge: impact of bias-correction method. Hydrol Earth Syst Sci Discuss 9:4989–5037. https://doi.org/10.5194/hessd-9-4989-2012

Rehana S, Mumjumdar PP (2013) Regional impacts of climate change on irrigation water demands. Hydrol Process 27:2918–2933. https://doi.org/10.1002/hyp.9379

Sentelhas PC, Gillespie TJ, Santos EA (2010) Evaluation of FAO Penman–Monteith and alternative methods for estimating reference evapotranspiration with missing data in Southern Ontario, Canada. Agric Water Manag 97:635–644. https://doi.org/10.1016/j.agwat.2009.12.001 2010.

Shahid S (2011) Impact of climate change on irrigation water demand of dry season *Boro* rice in northwest Bangladesh. Clim Change 105:433–453. https://doi.org/10.1007/s10584-010-9895-5

Sheff J, Frierson DMW (2012) Robust future precipitation declines in CMIP5 largely reflect the poleward expansion of model subtropical dry zones. Geophys Res Lett 39:1–6. https://doi.org/10.1029/2012GL052910

Silva CS, Weatherhead EK, Knox JW, Díaz JAR (2007) Predicting the impacts of climate change—a case study of paddy irrigation water requirements in Sri Lanka. Agric Water Manag 93:19–29. https://doi.org/10.1016/j.agwat.2007.06.003

Silveira C, Souza Filho SS, F de A, Costa, Cabral AAC SL (2013) Avaliação de desempenho dos modelos do CMIP5 quanto à representação dos padrões de variação da precipitação no século XX sobre a região Nordeste do Brasil, Amazônia e Bacia do Prata e análise das projeções para o cenário RCP8.5. Rev Bras Meteorol 28:317–330

de Souza Filho FA, Lall U (2004) Modelo de previsão de vazões sazonais e interanuais. Brazilian J Water Res 9:61–74. https://doi.org/10.21168/rbrh.v9n2.p61-74

Taylor KE, Stouffer RJ, Meehl GA (2009) A summary of the CMIP5 experiment design. http://cmip-pcmdi.llnl.gov/cmip5/docs/Taylor_CMIP5_design.pdf. Accessed 22 Jun 2017

Valverde P, Serralheiro R, Carvalho M de, Maia R, Oliveira B, Ramosa V (2015) Climate change impacts on irrigated agriculture in the Guadiana river basin (Portugal). Agric Water Manag 152:17–30. https://doi.org/10.1016/j.agwat.2014.12.012

Wada Y, Wisser D, Eisner S, Flörke M, Gerten D, Haddeland I, Hanasaki N, Masaki Y, Portmann FT, Stacke T, Tessler Z, Schewe J (2013) Multimodel projections and uncertainties of irrigation water demand under climate change. Geophys Res Lett 40:4626–4632. https://doi.org/10.1002/grl.50686

Woznicki SA, Nejadhashemi AP, Parsinejad M (2015) Climate change and irrigation demand: uncertain and adaptation. J Hydrol Reg Stud 3:247–264. https://doi.org/10.1016/j.ejrh.2014.12.003

Zamani R, Mohammad A, Ali A, Roozbahani A, Fattahi R (2016) Risk assessment of agricultural water requirement based on a multimodel ensemble framework, southwest of Iran. Theor Appl Climatol. https://doi.org/10.1007/s00704-016-1835-5